**Direct Research Journal of Chemistry and Material Science**
**Vol. 8, Pp. 31-43, 2021**
**ISSN: 2354-4163**
**DOI: https://doi.org/10.26765/DRJCMS0126893913**
**Article Number: DRJCMS0126893913**

**https://directresearchpublisher.org/drjcm**

*Full Length Research Paper*

# Corrosion Inhibition; and Antimicrobial Studies of Bivalent Complexes of 1-(((5-ethoxybenzo[*d*]thiazol-2-yl) Imino) methyl) naphthalene-2-ol Chelator: Design, Synthesis, and Experimental Characterizations

**Festus, C.[1]* and Wodi, C. T.[1,2]**

[1]Department of Chemistry, Ignatius Ajuru University of Education Rivers State, Nigeria.
[2]Community Boys Senior Secondary, Elelenwo, Port Harcourt, Rivers State, Nigeria.
Corresponding Author E-mail: festchi@yahoo.com

Received 13 October 2021; Accepted 25 November 2021; Published 30 November 2021

**ABSTRACT:** Heteroleptic bivalent complexes, [M(L)(Y)(Z) ($nH_2O$)] (M=$Mn^{2+}$, $Ni^{2+}$, $Cu^{2+}$and $Zn^{2+}$); L=1-(((5-ethoxybenzo[*d*]thiazol-2-yl)imino) methyl)naphthalene-2-ol (HL), Y=2,2'-bipyridine, Z= OAc, n=0,I,2) have been synthesized through reflux-condensation of 2-hydroxy-I-naphtaldehyde, 2-amino-6-ethoxybenzothiazole and 2,2'-bipyridine. The bivalent complexes were acquired on reflux of the -C=N-chelator with acetate salts of, Mn Ni, Cu, and Zn in ethanol ($CH_3CH_2OH$). Varied shades of colour distinct from the precursor reagents were noticed for the compounds. The HL plus its complexes were characterized via analytical (melting point, magnetic susceptibility ($\mu_{eff}$), molar conductance, plus solubility test) methods; spectral (Fourier Transformation Infrared (FTIR), electronic (UV-vis) assessments; corrosion inhibition plus antimicrobial evaluations. The FT-IR spectrum of HL presented a band at 1622$cm^{-1}$ which moved to 1616-1622 $cm^{-1}$ in the spectra of the complexes and was apportioned to an azomethine moiety. The complexes were spin-free as well as non-ionic in nature except the $Zn^{2+}$ complex. The compounds were found to be inactive against *Proteus mirabilis* but exhibited one form of action or the other against all other screened microbes. However, outstanding antifungal actions were acquired for the compounds against *Aspergillus flavus*, *fuserium sp.* and *Aspergillus Niger*. The -C=N-chelator plus its bivalent complexes also presented substantial corrosion inhibition behavior in opposition to corrosion of mild steel in aggressive HCl solution. The complexes had extra inhibition efficiency (IE) than the ligand.

**Keywords**: 2-amino-6-ethoxybenzothiozole, characterization, antimicrobial actions, corrosion inhibition, naphthaladehyde

## INTRODUCTION

Through the evolution and progressive development of science and technology, life on Earth progressively becomes easier and more liveable. Though science and technology continues to have its cons on life and living, its pros cannot be overemphasized as technological products and materials have been of enormous help in making life liveable and adaptable. Such technological outfits include industries, construction materials and machines. Mild steel (MS) has been found to be a chief material applied in these industries, construction materials and production of machines (Taghried et al., 2020; Nnenna et al, 2020). The acidic environment of hydrochloric acid is also widely used in industrial fields, such as pickling (rust removed from steel plates and rods), and cleaning operations, acidification of oil drilling in oil wells; plus, the regeneration of ion-exchange resins (Taghried, et al., 2020; Festus et al., 2019). Inasmuch as the acidic environment has important applicability in the industries, it however poses a major disadvantage in terms of corroding metallic sheets' surfaces, affecting the positive economic importance of these industrial processes. Thus, it becomes a major concern in the industrial field as to how to manage, reduce or even eradicate, where possible, this corrosive effect of the acidic solutions and mediums while adopted in useful industrial processes. Unfortunately, we are yet to find or produce a substance capable of terminating the corrosion process on metals by acidic or aquatic environment. However, one of the most effective and novel ways to protecting metals from corrosion in acidic environment is

the use of organic inhibitors. These organic inhibitors were originally gotten from plant extracts, but are now significantly produced from known chemical compounds, in addition to the involvement of different criteria, producing an anti-corrosion, inexpensive and environmentally friendly organic ligand (Taghried et al., 2020). Organic ligands containing oxygen and nitrogen donor atoms have contributed immensely to the development of coordination chemistry (Festus et al., 2018a). However, organic ligands containing sulphur heteroatom is the most functional as sulphur coordinates better than those containing oxygen and nitrogen. The adsorption of the organic ligand forms a tight protective film as layer on the MS surface and removes acid molecules from the steel surface (Al-Baghdadi et al., 2018; Kadhim et al., 2017). Hence, the synthetic organic ligands give light to the industries which utilize acidic mediums for their industrial processes. Recently as pointed out above, Schiff bases have gained significance as effective corrosion inhibitors of mild steels (Festus et al., 2020) in addition to their known special properties such as ability to form stable complexes (Hameed et al., 2015), high stability of their coordination compounds and good solubility in carbon-based solvents. The latter makes -C=N-chelators fit into a wide range of biological actions (antibacterial, antifungal plus anti-inflammatory (Halli et al., 2013, Osowole and Festus, 2015a), analytical applications (spectrophotometric determination of heavy metals (Kumar et al., 2009, Kumari and Chaudhary, 2014)) and as good scavengers of oxidative radicals owing to the presence of imine moiety, heterocyclic ring systems plus non-cyclic heteroatoms (Eissa, 2013) within their structural units. Propelled by the above and more, this study intends to design, synthesis, and experimentally characterize 1-(((5-ethoxybenzo[*d*]thiazol-2-yl) imino) methyl) naphthalene-2-ol chelator and it $Mn^{2+}$, $Ni^{2+}$, $Cu^{2+}$ and $Zn^{2+}$ complexes; and to evaluate them for corrosion inhibition plus antimicrobial potentials.

## Experimental

### Materials

All chemicals; 2-hydroxyl-1-naphthaldehyde, 2-amino-6-ethoxybenzothiazole, 2,2'-bipyridene, $Mn(OAC)_z4H_2O$, $Ni(OAC)_2.4H_2O$, $Cu(OAC)_2.H_2O$ $Zn(OAC)_2.2H_2O$, Zn-dust, were all acquired from Aldrich company Germany and used as supplied. The solvents used were of analytical grade.

### Instruments plus instrumentations

The elemental (C, H, N) compositions of the compounds were acquired on a Vario EL III. Volumetric titration was adopted to acquire percentage metal content in the l complexes, while an electronic conducting set HANNA HI 991 300 conductivity meter of 1.0 cell constant was adopted to acquire the molar conductance measurements in dimethylsulphuroxide in a $1x10^{-3}$ $moldm^{-3}$ solution of the bivalent complexes separately. Magnetic susceptibilities of the powdered complexes were examined on a Johnson mathey magnetic balance. Diamagnetic corrections were calculated on Pascal's constant basis. The infrared spectra of the ligand and its complexes were carried out on a PERKIN ELMER FI-IR SPECTRUM BX Spectrophotometer using KBr disc in the scale 4000-350$cm^{-1}$. The ultraviolet and visible spectra measurement of the ligands and its metal complexes were recorded on PekinElmer FT-IR-Lambda spectrophotometer within the scales; 190-400nm plus 400-900nm.

### Preparations

#### Preparation of 1-(((5-ethoxybenzo[*d*]thiazol-2-yl) imino) methyl) naphthalene-2-ol

The -C=N-chelator; 1-(((5-ethoxybenzo[*d*]thiazol-2-yl) imino) methyl) naphthalene-2-ol (Scheme 1) was prepared following a method seminar to that documented in literature (Kpee et al., 2018; Festus et al., 2019). 11.26g (0.058 mol) of 2-amino-6-ethoxybenzothiazole dissolved in 35 mL of $C_2H_5OH$ was stirred magnetically on drop-wise addition of 10.00g (0.058 mol) of 2-hydroxyl-1-naphthaldehyde pre-dissolved in 30 mL of $C_2H_5OH$. Four (4) drops of $CH_3CO_2H$ was added to the mixture and refluxed at 50–55$^oC$ (Figure 1). After 3 hours, the products were precipitated on freezing in ice, collected through filtration, rinsed using $C_2H_5OH$, recrystallized from warm $C_2H_5OH$ solution and dried over anhydrous $CaCl_2$.

#### Preparation of Heteroleptic Bivalent Complexes

The bivalent heteroleptic -C=N-chelator complexes were acquired according to scheme 1. Weighed mass of 1.1g of 1-(((5-ethoxybenzo[*d*]thiazol-2-yl) imino) methyl) naphthalene-2-ol was dissolved in 20 mL of $C_2H_5OH$. To this solution, an equivalent amount of 2,2'-bipyridine plus each separate metal salt was gradually added (Figure 2). The respective mixtures of individual metal were refluxed for 3 hr on adding 0.4 mL $N(C_2H_5)_3$ buffer with continuous stirring. Formed precipitates were collected by filtration, washed with hot $C_2H_5OH$ and dried oven $CaCl_2$.

### Corrosion inhibition studies

#### Mild steel coupons' preparation

Mild steel sheet acquired from Rivers State University of estimated compositions: 0.120%-C, 0.900%-Mn, 0.066%-

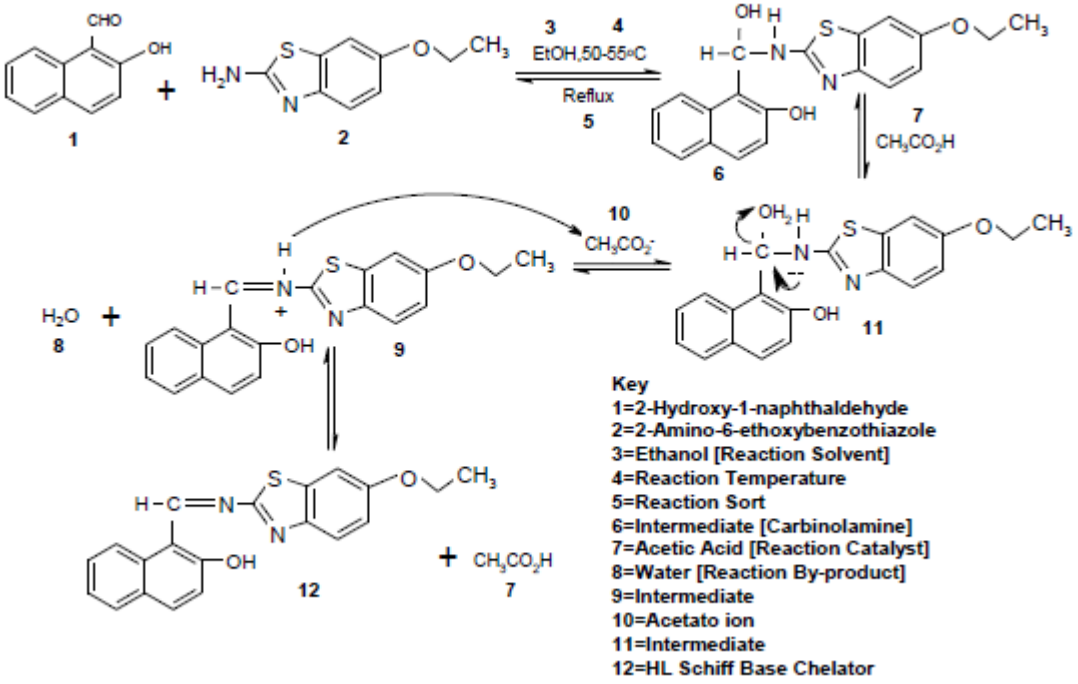


**Figure 1:** Synthesis of the Schiff base chelator.

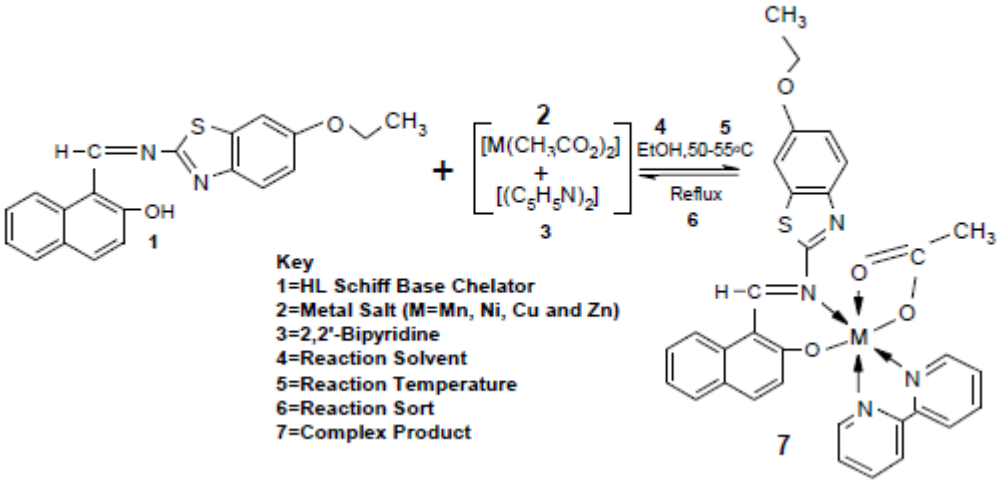


**Figure 2:** Synthesis of metal complexes

S, 0.050%-P, 0.1005%-Si plus 98.314%-Fe of 0.5 and 0.7mm thickness were cut into rectangular coupons of sizes 40mm x 40mm plus 40mm x 50mm. The coupons were mechanically refined with emery paper to acquire spotless glossy superficial, washed in distilled $H_2O$, degreased in $C_2H_5OH$, dehydrated in $CH_3COCH_3$ and kept in wet-free desiccators for further usage.

**Gravimetric measurements**

Aggressive 1M-HCl solution was made via dilution of 37% HCl with twofold distilled $H_2O$ inhibitor solutions at altered concentrations (100, 200,300,400 as well as 500 ppm) and were adopted for inhibition studies. The-C=N-chelator plus its bivalent complexes were prepared by

dissolving the required amount in 10 mL of suitable solvent. A 100 mL of 1M HCl deprived of inhibitor stood adopted as blank test solution. 100 mL capacity beakers separately branded 100-500 with each comprising of 1M-HCl solution were adopted for weight evaluations. While the first beaker served as blank, the others comprised -C=N-chelator plus its bivalent chelates at the varied concentrations and normal temperature. Afterwards, 40 mm x 4 mm x 0.5 mm sized mild steel coupons abraded via emery paper, cleaned with $C_2H_5OH$, $CH_3COCH_3$, and distilled $H_2O$ were dried, and weighed and immersed into the experimental solutions using glass hooks. The weights of each immersed coupon was determined at varied 3, 5 plus 9 hr time frame. At the expiration of each time duration, specimens stood detached, polished with emery papers, cleaned in twofold distilled $H_2O$, degreased with $C_2H_5OH$, dehydrated in $CH_3COCH_3$ and reweighed. The first plus last weightiness of each specimen were recorded and used to calculate the weight loss as follows:

$$\Delta w = \frac{m1 - m2}{A} \quad (1)$$

The corrosion rate (CR) was calculated from the following equation 2.

$$CR = \frac{xw}{DAT} \quad (2)$$

The proficiency of the inhibitor was appraised via Equ. 3

$$\text{Inhibition efficiency \% (IE)} = \frac{\Delta w_1 - \Delta w_2}{\Delta w_1} x100 \quad (3)$$

## Biological studies

The -C=N-chelator and its bivalent Mn, Ni, Cu plus Zn complexes were evaluated against gram-positive (*Staphylicoccus Epidermidis*, *Streptococcus Pneumoniae, Staphylicoccus Aureus*) plus gram-negative (*E. Coli*, *Proteus Mirabillis* and *Klebsiella Oxytoca*) strains for in-vitro antibacterial actions according to established procedures (Osowole and Festus, 2013; Festus et al., 2021). The nutrient agar medium sub-culturing of adopted isolates occurred at 37°C for 24hrs. The dishes were swabbed with the inocula of the strains, left for 15mins to adsorb unto the gel, and sample solutions filled into the 6 mm diameter wells drilled on the seeded agar dishes via a sterile cork-borer. The sample solutions were kept for 1 hour in the refrigerator for thorough circulation of the sample into the medium and these were then nurtured for 24 hours at 37°C before observing the inhibition zones. Antibacterial actions were expressed as inhibition diameter zones in millimeter (mm). Streptomycin was employed as control (Raman et al., 2001, Festus et al., 2020). The in-vitro anti-fungiform actions of the HL chelator plus its bivalent metal chelates were screened against *Aspergillus Flavus, fuserium Sp and Aspergillus Niger.* The potato dextrose agar remained adopted as culture media (Festus et al., 2018c). The data received were measured with the activity of miconaozole standard drug.

## RESULTS AND DISCUSSION

### Synthesis

Reflux reaction of 2-amino-6-ethoxybenzothiazole and 2-hydroxyl-1-naphthaldehyde gave the -C=N-chelator described as HL (Scheme 1). Further condensation of the chelator with $M^{2+}$ acetates of Mn(II), Ni(II), Cu(II) and Zn(II) gave the respective stable bivalent M(II) chelates (Scheme 2).

### Physiochemical data

The physicochemical data of the synthesized -C=N-chelator plus its bivalent chelates are summarized in Table 1. The data of the bivalent chelates were consistent with the general formulation $[M(L)(Y)(Z)]\ nH_2O$ ($M=Mn^{2+}$, $Ni^{2+}$, $Cu^{2+}$ and $Zn^{2+}$; $L=C_{20}H_{15}O_2N_2S$, Y=2,2'-bipyridine, Z= OAc n=0, I,2). The chelator and its $M^{2+}$ complexes were stable and coloured solids. The chelator exhibited insolubility in $H_2O$ but solubility in most carbon-based solvents (Table 2), while its complexes showed different levels of solubility in some carbon-based solvents (Table 2). Acquired molar conductance data fell amid 9.3-37.2 $ohm^{-1}cm^2mol$ which remained very low compared to the values expected for an electrolyte signifying non-ionic nature of the complexes (Table 1). The $\mu_{eff}$ results of all the chelates presented one of Paramagnetism or the other and conformed to octahedral assemblages for the chelates. Acquired analytical data confirmed with 1:1:1 molar ratio. The complexes exhibit higher melting points than the Parent-C=N-chelator suggesting higher thermal stability, formation plus purity. The molar conductance measurements of the metal chelate listed in (Tables 1 and 2) were in the range of 9.3-37.2 $\Omega^{-1}cm^2mol^{-1}$. The values designated the non-ionic nature of complexes (Huheey et al., 1993).

### FT- IR spectral data

The FTIR spectra afford commendable specifics regarding the features of the moieties in synthesized compounds. The characteristic stretching vibration modes concerning -C=N-chelator plus its bivalent complexes are described in (Table 3). Apportioning the FT-IR bands were made in match with spectra of chelates in literature on comparable structures (Hernandez -Molina and Hernandez-Molina and Mederos, 2003; Aliyu and Sani, 2012; Kiran et al., 2015;

**Table 1**: Physicochemical data of the -C=N-chelator and their bivalent complexes.

| Compound/ MF | Shade | M. Pt(c°) | Ohm$^{-1}$cm$^2$ mol$^{-1}$ | Yield % | μeff (B.M) | Molecular weight | Analytical/Found (Cal.d) % C | H | N | S | M |
|---|---|---|---|---|---|---|---|---|---|---|---|
| HL, $C_{20}H_{16}O_2N_2S$ | Yellow | 180 | - | 76.50 | - | 348.404 | 68.94 (68.79) | 4.62 (4.58) | 8.04 (8.10) | 9.20 (9.02) | - - |
| $MnC_{30}H_{30}O_6N_4S$ | Light brown | 185 | 14.7 | 47.20 | 6.0 | 653.588 | 58.80 (58.88) | 4.26 (4.19) | 8.57 (8.63) | 4.90 (4.96) | 8.40 (8.52) |
| $NiC_{30}H_{28}O_5N_4S$ | Dark brown | 235 | 28.2 | 50.50 | 3.3 | 639.344 | 60.11 (60.19) | 4.41 (4.39) | 8.76 (8.71) | 5.01 (5.06) | 9.18 (9.21) |
| $CuC_{30}H_{28}O_5N_4S$ | Dirty green | 220 | 21.9 | 45.05 | 2.3 | 644.174 | 59.66 (59.58) | 4.38 (4.41) | 8.69 (8.71) | 4.97 (4.98) | 9.86 (9.97) |
| $ZnC_{30}H_{28}O_5N_4S$ | Orange | 260 | 36.1 | 72.30 | 1.0 | 646.004 | 59.49 (59.56) | 4.36 (4.40) | 8.67 (8.77) | 4.96 (4.94) | 10.11 (10.18) |

**Table 2:** Solubility of the-C=N-Chelator plus bivalent complexes.

| Compound | Dist.$H_2O$ | $HCON(CH_3)_2$ | $(CH_3)_2SO$ | $CHCl_3$ | $C_3H_5OH$ | $CH_3OH$ | $CH_2Cl_2$ |
|---|---|---|---|---|---|---|---|
| $C_{20}H_{16}O_2N_2S$ | IS | SS | IS | SS | SS | SS | S |
| $MnC_{30}H_{30}O_6N_4S$ | IS | S | S | S | SS | SS | S |
| $NiC_{30}H_{28}O_5N_4S$ | SS | S | S | S | S | S | S |
| $CuC_{30}H_{28}O_5N_4S$ | SS | SS | SS | SS | SS | SS | SS |
| $ZnC_{30}H_{28}O_5N_4S$ | SS | S | S | S | SS | SS | S |

S=Soluble, SS=slightly Soluble, IS=Insoluble

**Table 3:** FTIR of the Mixed Ligand (HLB) and its bivalent complexes.

| Compounds | $C_{20}H_{15}O_2N_2S$ | $MnC_{30}H_{23}O_2N_4S$ | $NiC_{30}H_{23}O_2N_4S$ | $CuC_{30}H_{23}O_2N_4S$ | $ZnC_{30}H_{23}O_2N_4S$ |
|---|---|---|---|---|---|
| OH/$H_2O$ | 3337 | 3434 | 3437 | 3422 | 3433 |
| -C=N | 1622 | 1621 | 1620 | 1617 | 1618 |
| -C=C | 1601 | 1601 | 1602 | 1600 | 1601 |
| Aromatic C-N | 1232 | 1231 | 1212 | 1254 | 1230 |
| Stretch C-O | 1057 | 1058 | 1060 | 1066 | 1066 |
| C-H Stretch | 2926 | 2977 | 2978 | 2977 | 2975 |
| Aliphatic C-C | 1036 | 1036 | 1038 | 1041 | 1042 |
| C-S | 813 | 813 | 834 | 825 | 832 |
| C-C Stretch (n ring) | 1574 | 1574 | 1577 | 1573 | 1568 |
| =C-H Aromatic - | 748 | 3066 | - | - | 3058 |
| CH rocking in plane | | 743 | 749 | 745 | 744 |
| OH bending | 942 | 975 | 976 | 961 | 974 |
| =C-H Aromatic bend | | 942 | 942 | 946 | 942 |
| $CH_2$ in plane bending | 1450 | 1450 | 1453 | 1453 | 1456 |
| $CH_3$ bend - | | 1394 | 1383 | 1388 | 1378 |
| M-N | | 590 | 628 | 633 | 588 |
| M-O - | | 432 | 466 | 496 | 494 |

Osowole and Festus, 2015a; Festus et al., 2020). The band in the spectrum of the chelator at 1622 cm$^{-1}$ was apportioned to stretching vibration of the imine moiety (-C=N-), a confirmation of the formation of the -C=N-chelator. The band owing to the imine moiety was seen in the spectra of the bivalent complexes but at somewhat lesser wave-numbers amid 1617-1621cm$^{-1}$ indicative of the effect of chelation with the $M^{2+}$ ions (Sayed et al., 2020). Similarly, the bands arising from C=C function stood noticed in the spectra of the compounds at 1600-1602cm$^{-1}$ with comparable intensities to that of the C=N moiety. A broad band at 3337cm$^{-1}$ in the spectrum of the chelator was apportioned to vibration of the OH group, a common band associated with -C=N-chelators bearing hydroxyl groups (Aazam et al., 2006; Abel-Olaka et al., 2019). The latter appeared at slightly different frequencies (3393-3437) cm$^{-1}$ in the spectra of the bivalent complexes and were assigned to coordinated $H_2O$ molecules. The OH bending vibration observed at 942 cm$^{-1}$ in the spectrum of the chelator shifted to higher frequency 943-976cm$^{-1}$ confirming the existence of coordinated $H_2O$ molecules (Osowole and Festus, 2013). The aliphatic ν(C-H) band seen at 2926 cm$^{-1}$ in the spectra of the -C=N-chelator moved to 2975–2978 cm$^{-1}$in

**Table 4**: Electronic absorption spectra data of the mixed ligand metal complexes.

| COMPOUNDS | SOLVENT | ABSORPTION | BAND ASSIGNMENT | GEOMETRY |
|---|---|---|---|---|
| HL, $C_{20}H_{16}O_2N_2S$ | | 28,323 | | |
| | | 33784 | | |
| $MnC_{30}H_{30}O_6N_4S$ | $HCON(CH_3)_2$ | 39683 | $\pi - \pi^*$ | |
| | | 33,784 | $\pi - \pi^*$ | |
| | | 15576 | $^6A_{1g} \rightarrow {}^4T_{1g}$ | |
| | | 14728 | $^6A_{1g} \rightarrow {}^4T_{1g}$ | |
| $NiC_{30}H_{28}O_5N_4S$ | $HCON(CH_3)_2$ | 33784 | $\pi$-$\pi^*$ | Octahedral |
| | | 24876 | n-$\pi^*$ | |
| | | 18450 | $^1A_{1g} - {}^1B_{1g}$ | |
| $CuC_{30}H_{28}O_5N_4S$ | $HCON(CH_3)_2$ | 40161 | Charge Transfer | Octahedral |
| | | 33784 | $\pi$-$\pi^*$ | |
| | | 16,666 | $^2B_{1g}$ -$^2E_{2g}$ | |
| | | 14,771 | $^2E_g - {}^2T_{2g}$ | |
| | | 13,123 | $^2E_g - {}^2T_{2g}$ | |
| $ZnC_{30}H_{28}O_5N_4S$ | $HCON(CH_3)_2$ | 39,683 | $\pi - \pi^*$ | Octahedral |
| | | 33,784 | $\pi - \pi^*$ | |
| | | 27,548 | n – $\pi^*$ | |
| | | 18,553 | | |
| | | 16,077 | | Octahedral |
| | | 14,528 | | |

the spectra of the bivalent heteroleptic complexes but was accompanied by the presence of sharp and strong intensity bands around 1375–1394 $cm^{-1}$ consequently apportioned to C-H bending vibration (Aazam et al., 2006). The chelator exhibited strong intensity band at 1232 $cm^{-1}$ ascribed to the stretching mode v(C–N) of aromatic groups which appeared stronger in the spectra of the bivalent complexes, a consequence of the addition of 2,2'-bipyridine chelator during chelation (Festus et al., 2019). The chelator exhibited asymmetric bi-dentate behaviour coordinating with its imine nitrogen and deprotonated oxygen atoms to the bivalent metal ion. The latter were confirmed by the new bands at 590-671 $cm^{-1}$ and 414-496$cm^{-1}$ which were non-existent in the chelator and indicates $M^{2+}$ to nitrogen (M-N) and oxygen to $M^{2+}$ (M-O) bands.

## Electronic spectral plus $\mu_{eff}$ measurement

The electronic spectra of the chelator plus its bivalent complexes acquired in $HCON(CH_3)_2$ presented intra-ligand (n→**π**,*-**π**-**π***) and metal complexes (*d-d*; L-MCT/M-LCT) transitions, while acquired $\mu_{eff}$ data for the chelates remained separately suggestive of paramagnetism. The geometrical assignment to the metal complexes arose from the electronic absorptions plus $\mu_{eff}$ data (Osowole and Festus, 2013, Nevin and Kenan, 2018). The UV spectrum of the chelator (HL) presented two absorption peaks at 28323 and 33,784 $cm^{-1}$ allocated to n→**π** and **π**→**π*** transitions separately (Ajlouni et al., 2012, Taha et al., 2012, Festus et al., 2021). The peaks remained noticed at lesser $cm^{-1}$ (27548-24876 and 39683-33784 $cm^{-1}$) in the spectra of the bivalent complexes (Table 4) owing to chelation amid the chelator and metal ions (Festus et al., 2019). The heteroleptic $Mn^{2+}$ complex in its visible spectrum presented distinctive bands consistent of $^6A_{1g} \rightarrow {}^4T_2$ (G) and $^6A_{1g} \rightarrow {}^4E_g$ (G) transitions at 15576 $cm^{-1}$ and 14728 $cm^{-1}$ respectively. The bands conform with an octahedral assemblage apportioned to the $Mn^{2+}$ complex (Abdou et al., 2015; Osowole and Festus, 2015a). The experimental $\mu_{eff}$ value of 6.0 B.M substantiated the apportioned spin-free octahedral assemblage to the heteroleptic $Mn^{2+}$ chelate of $3d^5$ arrangement (Cotton et al., 2003) and conforms with the expected $\mu_{eff}$ values of 5.9–6.5 BM (Cotton et al., 1999; Osowole and Festus 2015b) for bivalent Mn chelates (Table 4).

The varied absorptions at 33784 $cm^{-1}$; and 24876-24876 $cm^{-1}$ noticed in the UV spectrum of the $Ni^{2+}$ chelate were attributed to aromatic ring (**π**–**π***) plus imine (n-**π***) moiety transitions separately. The diffused spectrum of the $Ni^{2+}$ chelate was characterized by threefold bands at 18.450 $cm^{-1}$, 15,723 $cm^{-1}$, and 14599 $cm^{-1}$ attributable to $^3A_{2g} \rightarrow {}^3T_{2g}(P)$, $^3A_{2g} \rightarrow {}^3T_{1g}(F)$, and $^3A_{2g} \rightarrow {}^3T_{1g}(F)$ transitions individually (El-Tabl et al., 2015; Osowole and Festus, 2015a). This assignment was consistent with high spin octahedral assemblage which was confirmed by the magnetic moment of 3.35 BM calculated for $Ni^{2+}$ complex and corresponds to magnetic moment values of 2.8-3.3 BM for nickel complexes since $\mu_{eff}$ value values of about or less than zero are acquired for square planer geometry due to their diamagnetic nature (Gaber et al., 1992). The synthesized $Cu^{2+}$ chelate had twofold bands observed at 40161 $cm^{-1}$ and 3784 $cm^{-1}$ typical of an M -L charge transfer and π – π* transitions. Additionally, three bands at 16666$cm^{-1}$, 14771$cm^{-1}$ and 13123$cm^{-1}$ were observed at the visible spectrum of the $Cu^{2+}$ complex and attributed to the electronic transitions; $^2B_1g \rightarrow {}^2E_2g$,

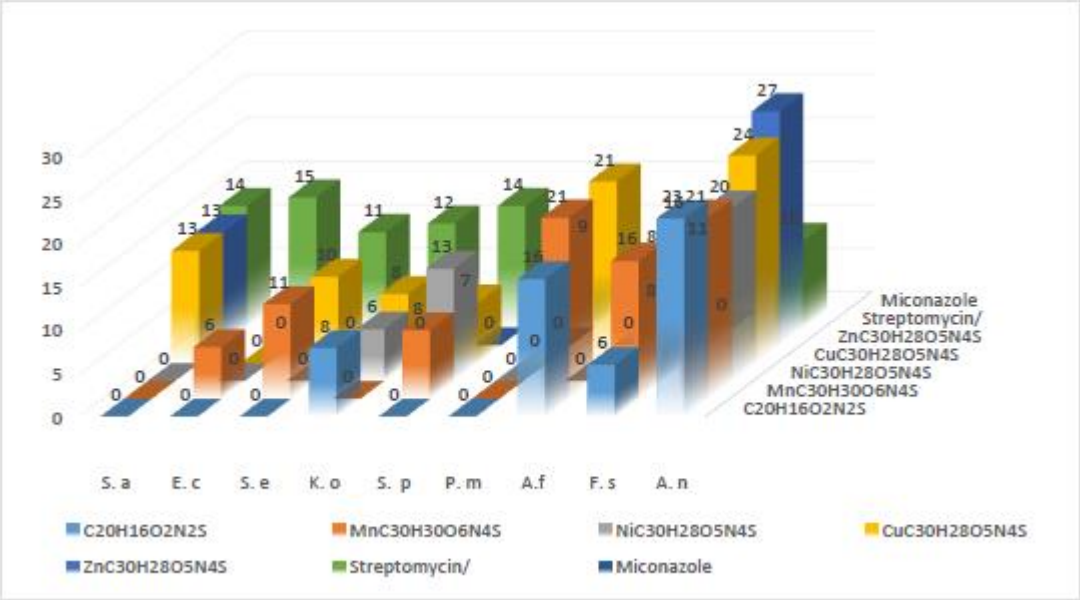


**Figure 3.** Anti-microbial Actions of the Heteroleptic Bivalent Complexes and their chelator

**Key:** *S.a=S. aureus; E.c= E.coil; S. e=S. epidermidis; K. o=K. Oxytoca; S.p= S. pneumoniea; P. m= P.mirabilis; A. f= A. flavus; F. s=F.Spices; A. n= A. niger*

$^2B_1g \rightarrow {}^2A_1g$ and $^2Eg \rightarrow {}^2T_ig$ respectively. This denotes John-Teller distortion of an octahedral geometry (Cotton et al., 2003). The absence of bands below 10000 $cm^{-1}$ indicates that tetrahedral geometry was not possible (Osowole and Festus, 2013). For facts about number of metal centers within a Cu-chelate, magnetic moment values stand helpful but not for geometry predictions. Mononuclear bivalent Cu chelates are estimated to parade moments of 1.9-2.2B.M or even higher values (Khalil et al., 2001) irrespective of geometry. Our $Cu^{2+}$ chelate assigned octahedral structural assemblage based on the support of the calculated $\mu_{eff}$ value of 2.3BM. Divalent $Zn^{2+}$ ion forms various complexes with different geometries. The $Zn^{2+}$ chelate ($ZnC_{30}H_{23}O_2N_4S$) displayed intra-ligand bands ($\pi - \pi^*$ and $n - \pi^*$) at 39683-33,784 $cm^{-1}$ and 27548 $cm^{-1}$.

## Biological data

The bivalent chelates of $Mn^{2+}$, $NI^{2+}$, $Cu^{2+}$ and $Zn^{2+}$ prepared from 1-(((5-ethoxybenzo[*d*]thiazol-2-yl) imino) methyl) naphthalene-2-ol were apprised against nine microbial strains for antimicrobial properties. Acquired zones of growth inhibition (results) are presented as (Figure 3) and conforms with literature reports that heterocyclic chelators bearing N, O, and S atoms exhibit broad spectrum antimicrobial actions against pathogenic microbes (Patel et al 2012; Festus et al., 2018c), but are more active upon chelation with metal ions (Huang et al., 2001). Streptomycin and miconazole were adopted as non-negative controls. The anti-bacteriological action results (Figure 1) denoted that all the tested complexes were active against all the bacteria species except *Proteus mirabilis* which failed to show any action. The data acquired were analyzed against the action of the standard anti-bacteriological drug, streptomycin. The chelator had activity only against *Klebiella oxytoca*. The heteroleptic bivalent complexes displayed better inhibitory effects against the bacterial strains than the parent imine chelator. The $Mn^{2+}$ chelate was active against all microbial species except *Staphylococcus Aureus* and *klebsiella oxytoca* with inhibitory zone ranges of 6-11mm. Our $Cu^{2+}$ was inhibited the growth of all the microbes with exemption of *E. Coil* with 7–13mm effects. The $Zn^{2+}$ complex presented inactivity against except against *staphylococcus Aureus* with inhibitory zone of 12.5mm. Furthermore, the $Ni^{2+}$ complex demonstrated activity only against *Klebsiella oxytoca* and *Streptococcus Pneumoniea* with inhibitory growth zone of 6-13 mm respectively. The enhanced anti-bacteriological action of the $M^{2+}$ complexes over their chelator agent might be expound on the basis of overtone concept (Festus et al., 2018b) plus tweedy's chelation theory (Thangadurai et al., 2001). The former proposes that the lipid membrane enveloping the cell allows the passage of only lipid-soluble materials due to hydrophobicity which is a considerable factor that controls the antimicrobial actions

**Table 5.** Effect of Time on CR on mild steel in 1M HCl solution of varied concentrations and constant temperature ($35^0$C) of the chelator.

| TIME (HRS) | CONC. | CR | % IE | Θ | ΔW |
|---|---|---|---|---|---|
| **9** | BLANK | 0.0044 | - | - | 0.0400 |
| | 100 | 0.0036 | 19.09 | 0.1909 | 0.0320 |
| | 200 | 0.0031 | 30.57 | 0.3057 | 0.0275 |
| | 300 | 0.0027 | 38.18 | 0.3818 | 0.0245 |
| | 400 | 0.0026 | 41.91 | 0.4190 | 0.0256 |
| | 500 | 0.0025 | 43.18 | 0.4318 | 0.0225 |
| 5 | BLANK | 0.0053 | - | - | 0.0265 |
| | 100 | 0.0042 | 20.75 | 0.2075 | 0.0210 |
| | 200 | 0.0038 | 28.30 | 0.2830 | 0.0190 |
| | 300 | 0.0007 | 86.79 | 0.8679 | 0.0035 |
| | 400 | 0.0004 | 92.45 | 0.9245 | 0.0020 |
| | 500 | 0.0003 | 94.34 | 0.9434 | 0.0015 |
| 3 | BLANK | 0.0050 | - | - | 0.0150 |
| | 100 | 0.0042 | 16.66 | 0.1666 | 0.0125 |
| | 200 | 0.0035 | 30.00 | 0.3000 | 0.0105 |
| | 300 | 0.0017 | 66.60 | 0.6660 | 0.0050 |
| | 400 | 0.0015 | 70.00 | 0.7000 | 0.0045 |
| | 500 | 0.0008 | 83.40 | 0.8300 | 0.0025 |

*CR = CR ( g/ cm2/h); IE (%); Θ – Degree of Θ*

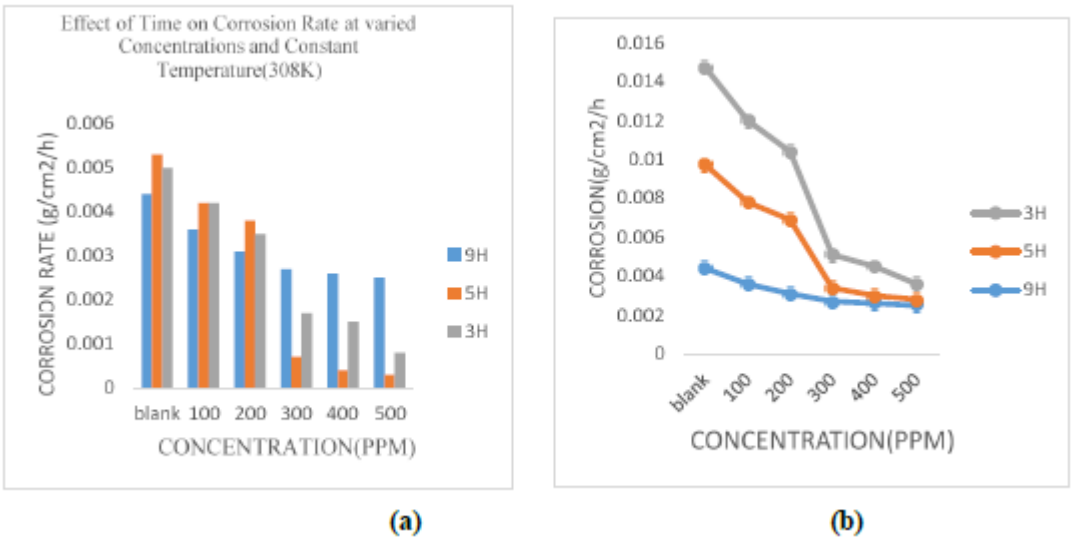


**Figure 4.** Effect of Time on Corrosion Rate [(a) and (b)] at varied Concentrations and Constant Temperature(308K).

(Thangadurai et al, 2001), whereas the latter holds that the polarity of the $M^{2+}$ion will be minimized to a greater extent due to overlap of the chelator's orbital and partial sharing of the positive charge(s) of the metal ions with donor groups (Thangadurai et al, 2001; Osowole and Festus, 2013). In addition, chelation increases the delocalisation of π-elections over the whole chelate ring enhanceing the lipophilicity of the chelates (Thangadurai et al, 2001). This enhanced lipophilicity fast-tracks the entering of the chelates into liquid membrances hence stopping the various metabolic actions of micro-organisms (Robertson, 1995). The increased action of the bivalent chelates can be channeled to the involvement of a $M^{2+}$ ion in standard cell workings (Osowole and Festus, 2015a). The synthesized chelator and its bivalent chelates also had anti-fugnal activity against *Aspergillus flavus, fuserium sp and Aspergillus niger* with good inhibition growth zones as shown in

**Table 6.** The weight, IE (%)plus CR acquired for a mild steel immersed in 100 to 500 ppm of 1M HCl solutions of a HL Chelator plus its complexes at 303k for 5hours duration.

| compound | CONC. | CR | % IE | Ɵ | ∆W |
|---|---|---|---|---|---|
| HL | BLANK | 0.0053 | - | - | 0.0265 |
| | 100 | 0.0042 | 20.75 | 0.2075 | 0.0210 |
| | 200 | 0.0038 | 28.30 | 0.2830 | 0.0190 |
| | 300 | 0.0007 | 86.79 | 0.8679 | 0.0035 |
| | 400 | 0.0004 | 92.45 | 0.9245 | 0.0020 |
| | 500 | 0.0003 | 94.34 | 0.9434 | 0.0015 |
| $Mn^{2+}$ | BLANK | 0.0066 | - | - | 0.0330 |
| | 100 | 0.0016 | 69.34 | 0.6934 | 0.0081 |
| | 200 | 0.0011 | 78.77 | 0.7877 | 0.0056 |
| | 300 | 0.00063 | 88.11 | 0.8811 | 0.0031 |
| | 400 | 0.0005 | 90.57 | 0.9057 | 0.0025 |
| | 500 | 0.0004 | 92.92 | 0.9292 | 0.0019 |
| $Ni^{2+}$ | BLANK | 0.0016 | - | - | 0.0081 |
| | 100 | 0.0010 | 37.50 | 0.3750 | 0.0050 |
| | 200 | 0.0009 | 45.31 | 0.4531 | 0.0044 |
| | 300 | 0.0006 | 60.94 | 0.6094 | 0.0031 |
| | 400 | 0.0004 | 76.56 | 0.7656 | 0.0019 |
| | 500 | 0.0001 | 92.18 | 0.9218 | 0.0006 |
| $Zn^{2+}$ | BLANK | 0.0056 | - | - | 0.0281 |
| | 100 | 0.0010 | 77.78 | 0.7778 | 0.0050 |
| | 200 | 0.0005 | 88.89 | 0.8889 | 0.0025 |
| | 300 | 0.0004 | 91.67 | 0.9167 | 0.0019 |
| | 400 | 0.0003 | 94.44 | 0.9444 | 0.0013 |
| | 500 | 0.0001 | 97.22 | 0.9722 | 0.0006 |

(Table 5). Aromatic -C=N-chelators containing the para-hydroxyls are known for moderate activities towards fungi strains (Hayashi, 2016). Hence, our chelator was found to be active against all the fungal strains (Victoria et al., 2010, Hayashi, 2016). The $Zn^{2+}$ chelate possessed the highest activity against all the fungi strains screened with inhibitory growth zone of 27mm *(Aspergillus niger)* even more significant than the standard drug adopted as a control. The chelates; $Ni^{2+}$, and $Zn^{2+}$ showed activities against *Fuserium spices* and *Aspergillus niger* with no activity observed against *Aspergillus flavus.* Also, HL chelator; $Mn^{2+}$, and $Cu^{2+}$ chelates presented activities against all the fungi strains used. The $Mn^{2+}$ chelate showed the highest actions with inhibitory zone of 21 mm and 16 mm against *Aspergillus flavus*, and *Fuserium spices* respectively.

## Corrosion inhibition studies

### Gravimetric measurements

The impact of –C=N-chelator plus its bivalent complexes on acid corrosion of mild steel in 1M HCl, gravimetric assessments of the mild steel was carried out in 100, 200, 300, 400, and 500 ppm of the compounds in a uniform solution at room temperature. A 100 ppm blank solutions without the compounds was also used as a control. The percentage IE plus CR acquired for the HL chelator from weight loss experimentations at 3, 5 and 9 hours are presented in (Table 5 and Figure 4). It could be noticed from the information that the HL-chelator plus its bivalent chelates had substantial corrosion inhibition behavior in opposition to corrosion of mild steel in a 1M HCl solution. The enhanced inhibition performance of the chelator perhaps could be due to coordination through the donor acceptors interplay among the non-chelated electron pairs of donor atoms of the chelator (Jacob and Parameswaran 2010, Nnenna et al., 2020). The $M^{2+}$ chelates presented extra IE than the free chelator. The enhanced efficiency of the bivalent chelates in comparison to the chelator could be credited to their bulky nature plus molecular planarity (Yiheyis et al., 2014). The calculated values of CR, Ɵ and IE from gravimetric evaluations at different concentrations of the studied inhibitor at constant temperature and varied time are summarized in (Table 6). The results denoted that CR decreases with increase in concentration. The decrease is a consequence of inhibitive influence of the chelator concentration. It might be seen from (Table 5) that IE ascended with increased chelator concentration yielding a value of 83.4%, 94.34% and 43.18% for 3, 5 and 9 hours separately at 500 ppm. This might be owing to the adsorption of HL chelator on the mild steel surface via free electron bonding pairs of N- and O- species plus pii-electrons of the cyclic rings joining alongside to the

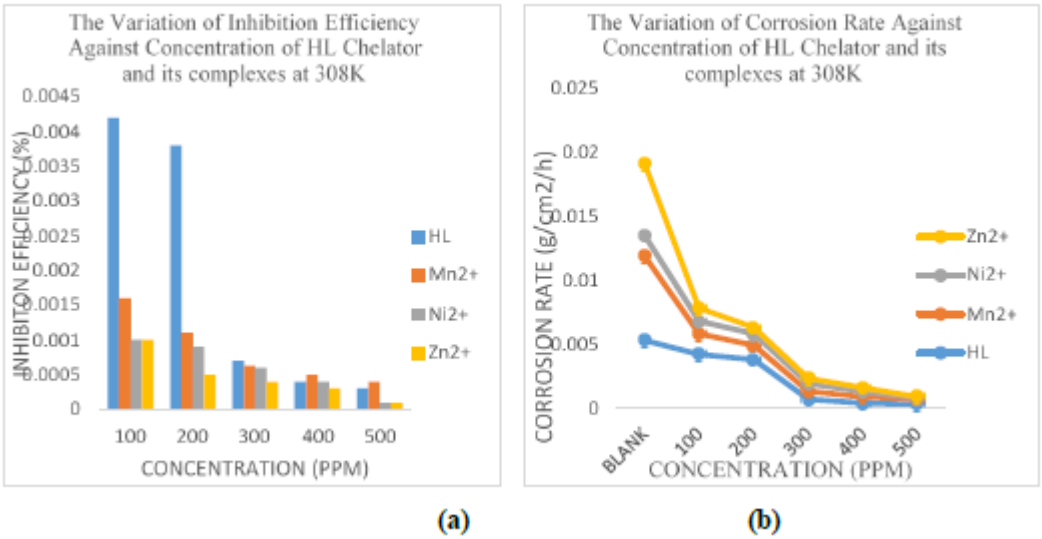


**Figure 5.** The Variation of Inhibition Efficiency [(a) and (b)] against Concentration of HL Chelator and its complexes at 308K

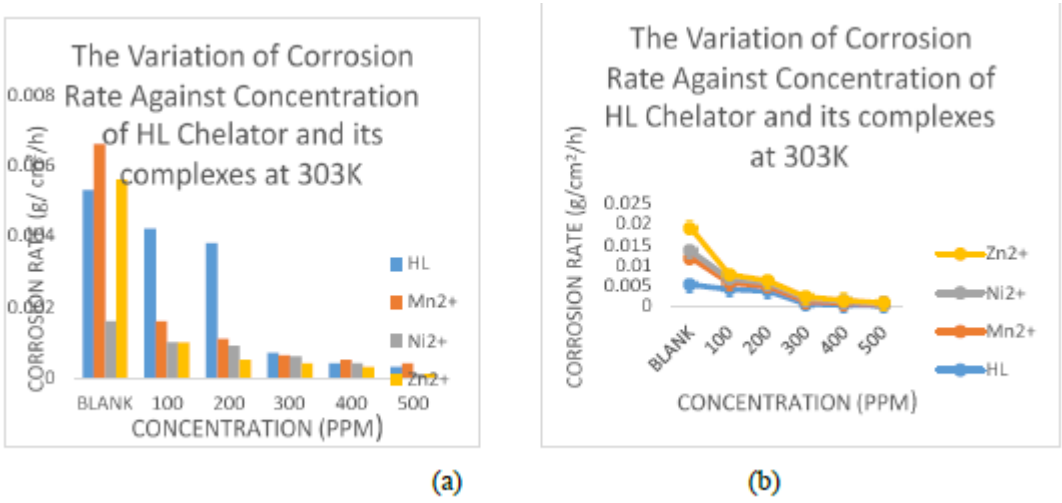


**Figure 6:** The Variation of Corrosion Rate against Concentration [(a) and (b)] of HL Chelator and its complexes at 303K.

imine moiety (N'guessan et al., 2021). The effect of time on corrosion rate at varied concentrations and constant temperature(308K) is showed in (Figure 4). The corrosion rate at different concentrations was affected by time of immersion of the steel in 1M HCl. The plot of corrosion rate agaisnt concentration indicated that rate of corrosion increases with increase in time. This decreases with increase in concentration of the HL and its bivalent complexes (Yiheyis et al., 2014). The plot of IE against concentration of the HL and its bivalent complexes is shown in (Figure 5). The result showed that increase in IE was consistent with rise in concentration of the compounds indicating that HL chelator and its bivalent complexes acted via establishment of a resistance layer surrounded by the $M^{2+}$ ion species and the corrosive medium by its adsorption on the mild steel surface (Nnenna et al., 2020, N'guessan et al., 2021). The heteroleptic bivalent chelates followed the order $Zn^{2+}$ > $Mn^{2+}$ > $Ni^{2+}$. This denoted that $Zn^{2+}$chelate had the highest IE (97.22%) whereas $Ni^{2+}$ with 92.18% had the least IE. The distinction inhibition performance was probably because of the difference in the steadiness plus

solubility of chelates in the acid solution (Mahendra, 2012). The inhibitory proficiency accelerated with improved concentration of the compounds (Figure 6). Better inhibition efficiency at higher concentration may be attributed to larger coverage of metal with inhibitor molecules (Mahdarian and Attar, 2009, Singh et al., 2013). This indicated that corrosion inhibition was an end consequence of adsorption of inhibitor on the metal surface plus the compounds acting as adsorption inhibitors (Mahendra, 2012). Improved IE at higher concentration can be ascribed to greater coverage of metal with inhibitor molecule (Taha and Ajilouni, 2012, Festus et al., 2020)

## Conclusion

Bivalent chelates of $Mn^{2+}$, $NI^{2+}$, $Cu^{2+}$ and $Zn^{2+}$ prepared from an imine (-C=N-) chelator; 1-(((5-ethoxybenzo[*d*]thiazol-2-yl) imino) methyl) naphthalene-2-ol have been characterized using analytical, spectral and theoretical techniques. The compounds were evaluated for biological and corrosion inhibition potentials. The different spectral techniques confirmed the formation of the chelates. An octahedral geometry was suggested for all the chelates. The low molar conductivity data gave credence to non-ionic nature of the chelates. The -C=N- chelator and its bivalent complexes had countless shades of colours distinct from the starting reagents. Acquired solubility data showed that the prepared compounds were soluble or slightly soluble in organic solvents but exhibited insolubility in $H_2O$. The FTIR spectrum of the chelator presented a band at 1622 $cm^{-1}$ which shifted to 1616-1621 $cm^{-1}$ in the bivalent chelates and was apportioned to -C=N- moiety, a confirmation of the formation of the chelator. This present study showed that bacterial species *strephylococus Epidermis* (21 mm) for the chelates have the highest values compared to other bacterial species and also have higher value than the value obtained from standard drug used. The highest antifungal activity (27mm) was recorded against *Aspergillus niger* for $Zn^{2+}$ complex. The $Mn^{2+}$ complex recorded highest actions of 21 mm and 16mm against *Fuserium Sp and A. flavus* separately. The influence of HL chelator plus its bivalent metal chelates on acid corrosion of mild steel showed they had considerable corrosion inhibition behavior in opposition to corrosion of mild steel in a 1M HCl solution. The chelates presented extra IE than the non-chelated chelator.

## ACKNOWLEDGEMENTS

The authors remain appreciative to the Department of Chemistry, Ignatius Ajuru University of Education Rumuolumeni, Rivers State for laboratory support equipment needed for the research work.

## Declaration of conflict of interest

The authors firmly say here that there is no existence of conflicting interest to this publication

## REFERENCES

Aazam, E.S., Fawazy, A., and Hitchcoek, P.B (2006). 4-methyl-7-(salicydeamino)coumarin, *Acta. cryst.,*

Abdou, S.E., moshira, M. A. E, Mohammed, A.W., and Nahia, A. E., (2015). Synthesis, characterization and anticancer of new metal complexes derived from (2-hydroxy-3-(hydroximino)-4-oxopenta-2-ylidene) benzohydrazine. *Bioinorganic. Chemistry Application*. 2015.126023, doi :10.1155/2015/126023

Abel-Olaka, L. C., Kpee, F. and Festus, C. (2019). Solvent Extraction of 3*d* Metallic Elements using $N_2O_2$ Schiff Base-Chelators: Synthesis and Characterization. *Nigerian Research Journal of Chemical Sciences.* 7(2); 133-146. *http://www.unn.edu.ng/nigerian-research-journal-of-chemical-sciences/p2*

Ajlouni, A. M., Taha, Z. A., Al-Hassan, A. K, and Anzeh, A. M. A. (2012). Synthesis, characterization, luminescence properties and antioxidant activity of ln(III) complexes with a new aryl amide bridging ligand. *Journal luminescence*, 132(6), 1357- 1363.

Al-Baghdadi, S. B. Hashim, F. G., Salam, A. Q.. Abed, T. K., Gaaz, T. S., Al-Amiery, *A. A.,* Kadhum, A. A. H., Reda, K. S. and , W. K.(2018). Synthesis and corrosion inhibition application of NATN on mild steel surface in acidic media complemented with DFT studies**.** *Results Phys,* 8 (2018), 1178-1184. https://doi.org/10.1016/j.rinp.2018.02.007

Aliyu, H. N., and Sani, U. (2012). Synthesis, characterization and biological activity of Mn(II), Fe(II), Co(II), Ni(II), and C-o(II). Schiff base complexes against multidrug resistant bacteria and fungi pathogens.*International Research Journal of pharmacy and Pharmacology,* 2,40 - 44.

Cotton, F. A., Wikinson, G., Murillo, C.A.,and Bochmann, M.(1999). Advance Inorganic Chemistry, 6th (ed). John Wilel,New York.

Cotton, F.A, Willikinson, G., Murilla C.A and Bochman. M., (2003). Advanced Inorganic Chemistry. 6th (ed). New york, NY:John Wiley and sons.
E62.04285-04287

Eissa, H., H. (2013). Synthesis and characterization of new azo-schiff bases and biological activity.

El-Tabl, A.S., Moshira M. A., El-Waheed, M. A., Wahba, N. A., El-Halim, A., El-Fadl, (2015). *Bioinorg. Chem. Appl*. 2015, 1 (2015). https://doi.org/10.1155/2015/126023

Festus, C., Ekennia, A. C. Ibeji, C. U. Okafor, S. N. Onwudiwe, D. C. Osowole, A. A. Ujam, O. T. (2018b). Synthesis, characterization, antimicrobial activity and DFT studies of 2-(pyrimidin-2-ylamino) naphthalene-

1,4-dione and its Mn(II), Co(II), Ni(II) and Zn(II) complexes. *Journal of Molecular Structure 1163 (2018) 455-464; https://doi.org/10.1016/j.molstruc.2018.03.025 0022-2860*

Festus, C., Ekennia, A. C. Osowole, A. A., Okafor, S. N., Ibeji, C. U., Onwudiwe, D. C., Ujam, O. T. (2018a). Synthesis, characterization, *in-vitro* antimicrobial properties, molecular docking and DFT studies of 3-{(*E*)-[(4,6-dimethylpyrimidin-2-yl) imino] methyl} naphthalen-2-ol and Heteroleptic Mn (II), Co(II), Ni(II) and Zn(II) complexes. *Open Chem.,* 2018; 16: 184–200. https://doi.org/10.1515/chem-2018-0020

Festus, C., Ekennia, A. C., Osowole, A. A., Olasunkanmi, L. O. Onwudiwe, D. C. and Ujam, O. T. (2018c). Synthesis, experimental and theoretical characterization and antimicrobial studies of some Fe(II), Co(II) and Ni(II) complexes of 2-(4,6-dihydroxypyrimidin-2-ylamino) naphthalene-1,4-dione. *Research on Chemical Intermediates 44(10):5857-5877; DOI 10.1007/s11164-018-3460-7*

Festus, C., Jude, I. A., Collins, U. I. (2021). Ligation Actions of 2-(3-hydroxypyridin-2-ylamino) naphthalen-1,4-dione: Synthesis, Characterization, *In-vitro* Antimicrobial Screening, and Computational Studies. *Indian Journal of Heterocyclic Chemistry*, 31(01); 1-13

Festus, C., Nnenna, O.W., and Moses, O. (2020). Preparation, spectral, characterization and corrosion inhibition studies of (E)-N-[(Thiophene-2-yl) methylene] pyrazine-2-carboxamide schiff base ligand. *Protection of Metals and Physical Chemistry of Surface*, 56(3), 651-662.

Festus, C., Odozi, W. N., and Olakunle, M. (2020). Preparation, spectral characterization and corrosion inhibition studies of (*e*)-*n*-{(thiophene-2-yl) methylene} pyrazine-2-carboxamide schiff base ligand. *Protection of Metals and Physical Chemistry of Surfaces.* 56(3); 651–662. **DOI:** 10.1134/S2070205120030107

Festus, C., Okafor, S. N. and Ekennia A. C. (2019) Heteroleptic Metal Complexes of a Pyrimidinyl Based Schiff Base Ligand Incorporating 2,2′ -Bipyridine Moiety: Synthesis, Characterization, and Biological Studies. *Front. Chem*. 7(862); 1-12. doi: 10.3389/fchem.2019.00862

Gaber, M., Mabrouk, H.E., and Ayad, M.M., (1992). Synthesis and characterization of Co(II), Ni(II), and Cu(II) complexes of salicyla -4-aminoantipyrirne and 2-hydrroxyl-naphthol-4-aminoantipyrine ‘and them adducts. *Monatshefte Fur Chemical/Chemical monthly*, 123, 1089 -1097.

Halli, R. S., Malipatil, R. B., and Sumathi, K. S., (2013). Scholars Research Library. *Der Pharmacia letter*, 2013, 5, 182.

Hameed, A., Al-Rashida, M., Uroos, M., Abid- Ali, S.,and Khan, K. M.( 2015). Schiff bases in medicinal chemistry: *A patient review*.*Expert Opinion on Therapeutic Patents*,27,63-79, http//doi.org/10.1080/13543776.2017.125275.

Hayashi M., (2016). Progress of chiral schiff base with carbon, synthesis in metal catalyzed asymetric Reaction of Chemical Reaction. *Electrochemical. Publications,* 16(6) ; 2708-2735 : doi:10.1002/ter201600091

Hernandez-Molina, R., and Mederos, A., (2003). Acyclic and macrocyclic schiff base ligands. *Comprehensive Coordination Chemistry, II*. 411-446.

Huang, Z., Lin, Z. and Huang, J. A., (2001). *Eur. J. Med. Chem*. 36, 863 https://doi.org/10.1016/S0223-5234(01),01285-5

Huheey J., Ellen A., Keiter and Richard I. (1993). Inorganic Chemistry, New York. 20

Jacob, K.S and Parameswaran, G., (2010). Corrosion all inhibition of mild steel in HCl solution by Schiff base furoin thiosemicarbazone. *International Journal of ChemTech Research*, 52, 224 - 228

*Journal of Current Research in Science,* 1, 444 - 450

Kadhim, A., Al-Okbi, A. K., Jamil, D. M., Qussay, A., Al-Amiery, A. A., and T. S. Gaaz, *et al.*(2017). Experimental and theoretical studies of benzoxazines corrosion inhibitors. *Results Phys,* 7 (2017), 4013-4019. https://doi.org/10.1016/j.rinp.2017.10.027

Khalil, S. M. E., Seleem, H. S., El-shetary, B.A., and Shebi, M. (2001). Mono- and bi-nuclear metal complexes of schiff base hydrazone(ONN) derived from O-hydroxyacetophenone and 2-amino-4-hyrazino-6-methylpyrimidine. Journal of Coordination Chemistry, 55,883-899, doi:10.1080/009589702000002213

Kiran, T., Prasanth, V.G., Balamurali, M.M., Vasari, C.S., Munuriami, P., Sathiyanarayartan, K.I., and Pathak, M .(2015). Synthesis spectroscopic, characterization and in vitro studies of new heteroleptic copper (II) complexes derived from 2-hydroxynaphthaldehyde Schiff’s bases and N, N donor ligands: Antimicrobial, DNA binding and N,N donor cyotoxic investigations. *Inorganical Chemical Acta,* 433, 26 – 34

Kpee, F., Ukachukwu, C. V. and Festus, C. (2018). Synthesis, Characterization and Extractive Potentials of Aminopyrimidine Schiff Base Ligands on Divalent Metal Ions. *Nigerian Research Journal of Chemical Sciences.* 4(2); 193-203. *http://www.unn.edu.ng/nigerian-research-journal-of-chemical-sciences/193*

Kumar, R. P., Chaudhary, (2010). A new profile of azomethines containing halogen and cyanoethyl moieties towards synthetic and pharmacological utilities. *Der ChemicaSinica*, 1, 55.

Kumar, S. D., Nath D., and Saxena, P. N. (2009). Applications of metal complexes of Schiff bases. *Journal of Scientific and Industrial Research*, 68(3), 181-187. http://hdl.handle.net/123456789/3170

Kumari S.,and Chauhan G.(2014). New cellulose- lysine Schiff-base-based sensor-adsorbent for mecury ions. *ACS applied Materials and Interfaces*, 6(8), 5908- 5917

Mahdarian, M., and Attar, M.M., (2009). Electrochemical behavour of some transition metal acetylacetonate

complexes as corrosion inhibitors for mild steel. *International Journal of ChemTech Research*, 51, 409 – 414

Mahendra, Y., (2012). Synthesis, Characterization and Biological activity of some transition metal complexes of N-Benzoyl-N-Z-thiophene thiocarbohydrazide. *International* Journal of Inorganic Chemistry, (8), https//doi.org/10.1155/2012/269497

N'guessan Y. S. D., Nagnonta H. C., Ollo K., and Albert T. (2021). Experimental and theoretical investigations on Copper corrosion inhibition by cefixime drug in 1M HNO3 solution. *Journal of Materials and Chemical Engineering, 9,11-28. https://www.scirp.org/journal/msce*

Nevin, T.,and Kenan,B., (2018). Synthesis., characterization and antioxidant activity of schiff base and its metal complexes. *European Journal of Chemistry,* 22-29.

Nnenna, W. O., Festus, C. and Muhammed, A. D. (2020). Synthesis, adsorption and inhibition behaviour of 2(thiophen-2-ylmethylidene) aminespyridine -3-olon mild steel corrosion in aggressive acidic media. *Nigerian Research Journal of Chemical Sciences.* 8, (2); 291-307. http://www.unn.edu.ng/nigerian-research-journal-of-chemical-sciences/ 291

ONS/ONO donor atoms and their biocidal activities. *Transition Metal Chemistry*, 26(6), 717- 722

Osowole, A. A. and Festus, C. (2015b). Synthesis, spectral magnetic and antibacterial studies of some divalent metal complexes of 3- {[(4,6-dihydroxy pyrimidin-2-yl) Amino]methyl}Napthalen-2-ol. *Journal of Chemical, Biological and physical sciences, **6**(11).*

Osowole, A. A. and Festus, C. (2013). Synthesis, characterization and antibacterial activities of some metal(II) complexes of 3-(-1-(2-pyrimidinylimino) methyl-2-napthol. *Elixir Appl. Chem. 59 (2013) 15843-15847*

Osowole, A. A. and Festus, C. (2015a). Synthesis, characterization, antibacterial and antioxidant activities of some heteroleptic Metal(II) complexes of 3-{[-(pyrimidin-2-yl) imino] methyl}napthalen-2-ol. *J. of Chemical, Biological and Physical Sciences*. 6(1); 080-089.

Patel, M. N., Joshi, H. N. and Patel, C. R. (2012). *Polyhedron 40*, 159 (2012). https://doi.org/10.1016/j.poly.2012. 03.050

Raman, N, Kulansamy, A, Slunmugasundaram, A., and Jeyasubramamian, K. (2001). Synthesis, Spectral, Redox and Antimicrobial Activities of Schiff Base Complexes derived from 1– phenyl– 2, 3 – dimethyl – 4 – aminipyrazol – 5 – one and acetoacetanilide. *Transition Metal. Chemistry,* 26, 131 – 135.

Sayed, S. S., Dawood, S., Ibrahim, K., Sajjad, A., Umar, A., and Atiqur, R. (2020). Synthesis and antioxidant activities of schiff bases and their complexes. *Biointerface Research in Applied Chemistry*, https://doi.org/10.33263/BRIAC106.69366963

Singh P., Singh A.K., and Singh V, P, (2013). Synthesis and corrosion inhibition properties of some transition metal (II)complexes with o-hydroxyacetophenone-2-thiophenoyl hydrazone, polyhedron. *International Journal of ChemTech Research*. 65,73 - 81

Taghried, A. S., Qusay, A. J., Mohammed, A. M. H,, Ahmed, A. A., Lina, M. S., Abdul, A. H. K. and Mohd, S. T.| (2020). New environmental friendly corrosion inhibitor of mild steel in hydrochloric acid solution: Adsorption and thermal studies, Cogent Engineering, 7:1, 1826077, DOI: 10.1080/23311916.2020.1826077.

Taha, Z.A.,and Ajilouni A.M., (2012). Synthesis, characterization, luminescence properties and antioxidant activity of mn(III) Complexes with a new Aryl Amide Bridging Ligand. *Journal of Luminescence*, 132(6), 1357- 1363

Thangadurai, T. D., and Karuppannan N., (2001). Tridentate Schiff base complexes of ruthenium(iii) containing

Victoria, K.J., Ku, S., and Nair, M.K., (2010). *Research Journal Pharmaceutical Biological Chemistry,* 101,32

Yiheyis, B. Z., Nithyakalyani D., and Ananda K.S., (2014). Synthesis, Structural Characterization, Corrosion inhibition and in vitro antimicrobial studies of 2-(5-methoxy-2-hydroxybenylideneamino) phenol Schiff base ligand and its transition metal complexes. *International Journal of ChemTech Research*, 6(11), 4569- 4578.